Hindawi
International Journal of Chemical Engineering
Volume 2022, Article ID 7952197, 10 pages
https://doi.org/10.1155/2022/7952197

Research Article

Experimental Analysis and Improvements of a Visible Spectrophotometer for Detection of Nano Materials

Pamula Rajakumari,[1] **Polaiah Bojja**,[2,3] **Smitha Chowdary Ch**,[4] **Sunkara Teena Mrudula**,[5] **Krishnam Raju Putta**,[6] **and Amsalu Gosuadigo**[7]

[1]*Department of Mathematics, Institute of Aeronautical Engineering, Hyderabad 500043, India*
[2]*Department of ECE, Koneru Lakshmaiah Education Foundation, Guntur 522502, A.P., India*
[3]*Institute of Aeronautical Engineering, Hyderabad, Telangana, India*
[4]*Department of CSE, Koneru Lakshmaiah Education Foundation, Vijayawada 522502, India*
[5]*Department of ECE, DVR & Dr. HS MIC College of Technology, Kanchikacherla, Vijayawada, India*
[6]*Department of Mechanical, Parul University, Vadodara, Gujarat, India*
[7]*Center of Excellence for Bioprocess and Biotechnology, Department of Chemical Engineering, College of Biological and Chemical Engineering, Addis Ababa Science and Technology University, Addis Ababa, Ethiopia*

Correspondence should be addressed to Pamula Rajakumari; rajakumari258@gmail.com, Krishnam Raju Putta; krishnamraju.putta@paruluniversity.ac.in, and Amsalu Gosuadigo; amsalu.gosu@aastu.edu.et

Received 27 December 2021; Revised 1 February 2022; Accepted 14 February 2022; Published 14 June 2022

Academic Editor: G.L. Balaji

As the field of nanotechnology advances, there is an increasing need for green nanomaterial identification devices. Recently, a few new studies have reminded us that as nanotechnology gets better and better, so will natural phenomena. As we grow closer to and finally reach the nanoscale, it is feasible that new physical expertise will develop. Developments in the future may allow for new technical advancements. It is the ability of nanotechnology to construct human constructs at the nanoscale that distinguishes it from other fields of science and engineering. Various components, including high-dissociation electron microscopy, centre-ion beam milling tools, and scanner probes, have made this practical. Spectrometers, sometimes known as spectrometers, are used in fabric identification machines. To conclude this inquiry, a nanoparticle scatter spectrometer was devised and built artificially. This study focused on the visible spectrum of spectroscopy because there are a broad number of programmes available for visible optical instruments.

1. Introduction

The importance of oblique tests in modern physics cannot be overstated, and infrastructure standards and best practises are typically based on them. Today's cutting-edge technology developments and discoveries have important implications and knowledge gained. For measuring and studying our natural world, the optical device software has proven to be an excellent instrument, according to these studies. When it comes to light-related events, our brains are already well versed in comprehending and processing them, no matter how many times we magnify the shape to be investigated. Because of this perceptual capacity, seeing optics and optical techniques in the same light as physical treasures and equations is exciting. To gather information on the structure and dynamics of the material, optically generated electron transitions and fabric vibrations can be employed to undertake complex and pleasant manipulation in the quantum mode. [1] Natural nanostructures are being studied in a similar way to strong-country systems [1] because of these remarkable spectroscopic properties.

Optical and electrical components go into the construction of seen spectrometers. There are many commercially available organised-made digital components that can be used in place of optical ones. Optical spectrometers are made up of four or five fundamental parts. The optical spectrometer features a few unique optical elements as well as diffusion-stimulating accessories such as pattern boxes, wavelength preference tools, and radiation power supervisors for parallelising, focusing, and orienting electromagnetic radiation.

Optics has a few basic concepts that can be utilised to generate several extended equations based on the same fundamental principles. One-of-a-kind criteria are used to evaluate optical materials and spectroscopy structures. In addition to the survival rule and pondered picture and diffraction recommendations, as well as absorption standards, there are other more guidelines and suggestions [2].

2. Proposed Research

2.1. Ray Optic and Wave Optics. To be consistent, we have to narrow down the ever-present principle to a more specific definition. Since dispersion and interference are not present, the ray optic must be converted to an optical wave. It is much easier to detect diffraction and interference if the object or gate being illuminated is of the same wavelength as the light that is being used to illuminate it. The wave will have the same impact as long as d equals the ray's behaviour. Imagining things this way might help

$$\sum_{\gamma/d \longrightarrow 0} \lim (\text{wave optices}) = \text{ray optics}. \tag{1}$$

2.2. Scattering by Dipoles Induced in Small Scatterers. Flat waves that are monochrome and do not have many colours would usually hit scatterers. For the sake of making things easier, we will treat the rest of the situation as $\varepsilon r = \mu r = 1$. In this case, if the incidence direction is defined by a n unit vector, the polarisation vector is

$$E_{inc} = \epsilon_0 E_0 e^{ikn.X}, \tag{2}$$

$$H_{inc} = n_0 \times \frac{E_{inc}}{Z_0}, \tag{3}$$

where $k = \underline{\omega}$ and a temporal dependence is perceivable as $e{-}i$. T. It is possible that these fields will make some small scatterers have p and m dipolar c moments, and those dipoles may want to spread the strength in all directions. In places where the scatterers are not near, the scattered discipline could be found as follows:

$$E_{sc} = \frac{1}{4\pi\epsilon_0} K^2 \frac{e^{ikr}}{r} \left[(n \times p) \times n - n \times \frac{m}{c}, \right. \tag{4}$$

$$H_{sc} = n \times \frac{E_{sc}}{Z_0}. \tag{5}$$

It says that n is the unit vector in the path of comment and r is the distance from where the comment is being spread out. The scattering differential move-segment is a quantity that has surface dimensions in the unit of spatial mind-set. It is called the scattering differential move-segment because it has surface dimensions in the unit of spatial mind-set:

$$\frac{d\sigma}{d\Omega}(n, \varepsilon; n_0, \varepsilon_0) = \frac{r^2 1/2 Z_0 \left|\varepsilon^*.E_{sc}\right|^2}{1/2 Z_0 \left|\varepsilon_0^*.E_{sc}\right|^2}. \tag{6}$$

By substituting E_{sc} and E_{inc} in (6), we have

$$\frac{d\sigma}{d\Omega}(n, \varepsilon; n_0, \varepsilon_0) = \frac{k^4}{(4\pi\varepsilon_0 E_0)^2} \left| \varepsilon^*.p + (n \times \epsilon^*).\frac{m}{c} \right|^2. \tag{7}$$

2.3. Scattering at Short Wavelengths. Probably, the other limit of scattering in long wavelengths proportional to the scatterer comes from the way we think about rays, like Kirchhoff's diffraction place, and show screen diffraction. It might be possible to back up these theories by limiting scattering to an angle that is just above the geometrical optics route. The idea of diffraction should be looked at when there is a thin, flat obstacle. For other types of boundaries, our calculations of scattering domain names are likely to be based mostly on Es and BS scattering fields. According to this, the following equation is probably written as follows:

$$\varepsilon^*.\mathrm{F}(\mathrm{k}, K_0) = \frac{i}{4\pi} \int \oint_{s1} -ek.x' \cdot \left[\omega\varepsilon^* (n' \times B_s) + \varepsilon^*.(k \times (n' \times E_s))\right].da'. \tag{8}$$

It is best to look at the shadow region's share on its own because of its generality. As a result, it can be reworked:

$$\varepsilon^*.\mathrm{F} = \varepsilon^*.F_{sh} + \varepsilon^*.F_{ill}. \tag{9}$$

For a flat wave with a k-wave vector and no polarisation,

$$E_i = E_0 \varepsilon_0 e^{ikx}, \tag{10}$$

$$B_i = k_0 \times \frac{E_i}{k}. \tag{11}$$

Considering

$$ik \cdot x' [\omega\varepsilon * \cdot (n' \times \mathrm{B}) + \varepsilon * \cdot (k \times (n' \times \mathrm{E}))]da',$$

$$\varepsilon^* \cdot F(k, k) = i \oint e^{-ik \cdot x'} [\omega\varepsilon * \cdot (n' \times \mathrm{B}) + \varepsilon * \cdot (k \times (n' \times \mathrm{E}))]da'. \tag{12}$$

$$\epsilon^*.F(K, K_0)_{sh} = \frac{E_0}{4\pi i} \oint e^{i(k_0 - k).x'} \epsilon^* .[(n' \times (K_0 \times \epsilon_0)) + k \times (n' \times \epsilon_0)da'], \tag{13}$$

$$\epsilon^*.F(K, K_0)_{sh} = \frac{E_0}{4\pi i} \oint e^{i(k_0 - k).x'} \epsilon^* .[(K + K_0) \times (n' \times \epsilon_0) + (n'.\epsilon_0)k_0]da'. \tag{14}$$

Short-wavelength limits: The sizes of k. x' and k_0. x' are bigger than one for these limits. In the above equation, the exponential factor should quickly change. This could make the integrator have a small mean, except for its forward kind

in which $k \cong k$. In the forward region of $\theta \leq K^1$, the second sentence is negligible in comparison $0\overline{kR}$ with the first sentence because $\varepsilon * k_0$ is from $\sin\theta << 1$ order. Because $\varepsilon * . k \equiv 0$,

$$\varepsilon^* . F_{sh} \cong \frac{iE_0}{2\pi}\varepsilon^* . \varepsilon_0 \int_{sh} e^{i(k_0-\kappa)x'} (k_0 . n')da'. \tag{15}$$

Polarisation Current [3]: Atomic and molecular spectroscopy is hampered by the polarisation problem. This is because the polarisation problem reveals the identity of alarming levels.

Atoms find their way into Maxwell equations through polarisation current, that is,

$$\nabla \times H = i_{c+n^2}\varepsilon_0 \frac{\partial E}{\partial t} + \frac{\partial P_a}{\partial t}, \tag{16}$$

where i_c is the conduction current that is carried by load carriers. $\eta^2\varepsilon_0\partial E/\partial t$ is the displacement current, which are addition to being affected by the host network in which active atoms are embedded, and $\partial P\ a$ is the polarisation current for activated atoms.

In case the environment's refractive index would be homogenous and we would neglect the conduction current, we have

$$\nabla . (\nabla \times H) \equiv 0 = n^2 \varepsilon_0 \frac{\partial}{\partial t} (\nabla . E) + \frac{\partial}{\partial t}\nabla . P_a, \tag{17}$$

$$\nabla . E = -\frac{1}{n_0\varepsilon_0} \nabla . P_a, \tag{18}$$

$$\begin{aligned} \nabla \times [\nabla \times E] &\equiv \nabla (\nabla . E) - \nabla^2 E = -\mu_{0\,(\partial/\partial t)} \nabla \times H \\ &= -n^2 \mu_0 \varepsilon_0 \frac{\partial^2 E}{\partial t^2} - \mu_0 \frac{\partial^2 p_a}{\partial t^2}, \end{aligned} \tag{19}$$

$$\nabla^2 E - \frac{n^2}{c^2}\frac{\partial^2 E}{\partial t^2} = \mu_0 \frac{\partial^2 p_a}{\partial t^2} - \frac{1}{n^2\varepsilon_0} - \nabla (\nabla . P_a). \tag{20}$$

2.4. Lasers. Coherent and focused light is produced by lasers, which are light-emitting diodes with the ability to produce a single colour of light. Because of this, spectroscopy can benefit greatly from its utilisation. Using "stimulation emission," a laser can be generated. In a two-level system, population inversion between the two levels is necessary for a stimulated emission from a higher energy level to dominate absorption. In order to alter the normal population distribution, pumping is a strategy in which energy is used to consume it. The term "active environment" refers to a system that incorporates population inversion and can exist in the solid, liquid, or gas phase. Lasers benefit from the dynamic environment that lies between the two mirrors. A minor amount of radiation leakage is present in one of the mirrors, despite its great reflecting capacity. The "laser cavity" is the area between the two mirrors. There must be an integer multiple of the half-wavelength distance between the two mirrors. A variety of dielectric materials, including SiO_2 and TiO_2, are applied to the mirrors' reflector surfaces. This is done to ensure that mirrors are nearly completely reflective at a particular wavelength. The reflectivity of standard aluminium, silver, or gold coatings is insufficient. It would be possible to cover one of the mirrors and emit light with an incidence ranging from 1% to 10% (radiation).

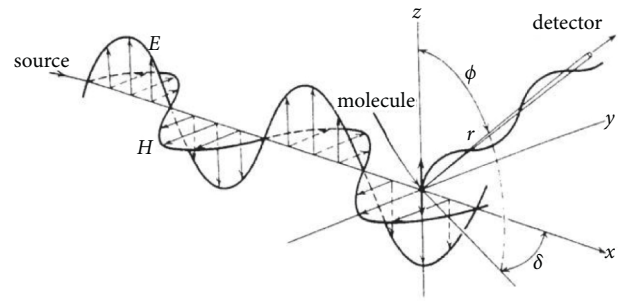

Figure 1: Molecular scattering of flat polarised light. Dipole 2 d in the direction of the z-axis for isotropic induction [4].

2.5. Scattering Spectroscopy. A "scattering spectrometer," sometimes known as a "nephelometer," is a device that monitors the scattering of optical rays through a substance. Each laser or lamplight can be used to characterise this device. The ones spectrometers use are solid-state detectors. Chemical substances and contaminants that could behave as pathogens if placed in water are detected using these spectrometers, which are widely used in wastewater treatment facilities. Some of these detectors appear to be cost-competitive for small R&D organisations. Semi-automated scattering spectrometers were used in modern-day research.

Measurement of dispersed light from solutions using a device [4]. Traditional electromagnetic principles can be used to calculate mild scattering from a single molecule:

It is therefore impossible for mild to be dispersed over the z-axis course. Figure 1 depicts the z-axis course dependency of polarised incident light scattering. The Z-axis path has no scattering. In scattering investigations, unpolarised light is the most commonly used. By measuring the intensity of two perpendicularly polarised beams of light, one can learn about the angular dependency of an isotropic molecule (in comparison with mild's wavelength). The following are the actual effects on scatterer intensities as a result of this:

$$\frac{i}{I_0} = \frac{\pi^2 a^2}{2\varepsilon_0^2 r^2 \lambda^4}\left(1 + cos^2\theta\right), \tag{21}$$

the angle at which many of the incident beams and announcements are oriented. An example of this angular dependence is shown in Figure 2-five-b. There are no differences between direct and inverse instructions when it comes to the intensity of dispersion. Scattered moderate intensity is inversely related to the wavelength implemented. As a result, the blue light is likely to be more dispersed than the red light, which means that the crimson colour of the suspended debris is more likely to be observed [5].

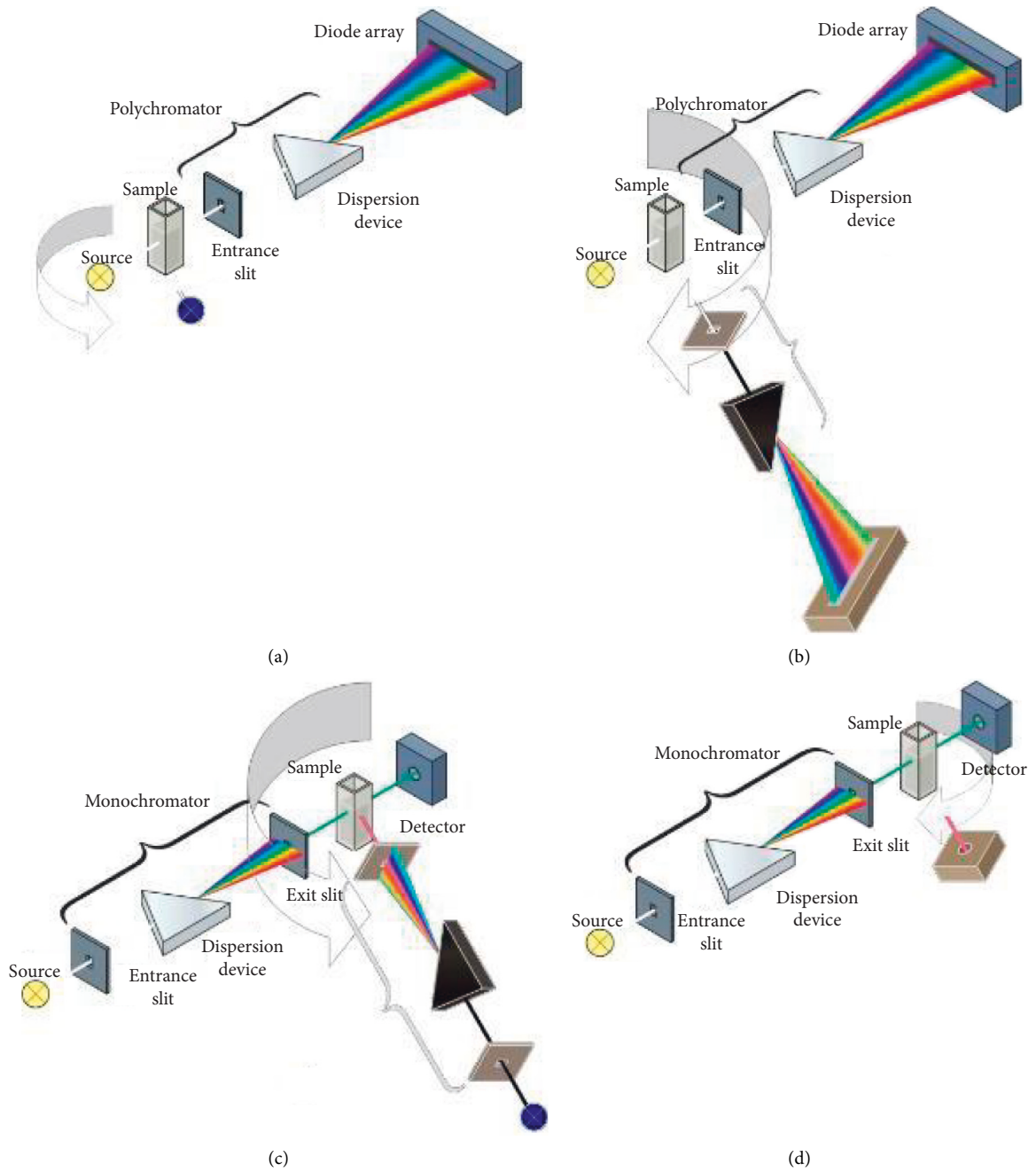

Figure 2: Scattered light is gathered by three revolving prisms, which route the scattered light to the detector. Devices are designed with a central pattern in mind [7].

$$\frac{i}{I_0} = \frac{\pi^2 a^2}{2\varepsilon_0^2 r^2}\left(1 + cos^2\theta\right). \tag{22}$$

By using polymer molecules in solution, we may determine scattering by accounting for the awareness variations in small quantities of pollution, smaller than a cube with wavelength-matched dimensions, which allows it to accommodate a substantial number of molecules. Advanced light scattering articles are buried in the manual's calculations section. This article proposes a less demanding method that is less concerned with statistical averaging yet yields more accurate results. [∗] results the refractive index, n, can be correlated with the polarisation of the polymer n, as well as the n_0 refraction index of the herbal solution:

$$n^2 - n_0^2 = \frac{N\alpha}{\varepsilon_0}, \tag{23}$$

where N is the number of polymer particles in a unit volume of the same size. When this equation is written down, it can be thought of as some way to say the polarisation equation based on how things have changed over time of a special refractive index, that is,

$$dn = n - \frac{n0}{dc}, \tag{24}$$

where c is the concentration per mass in unit volume and M is the molar mass of the polymer.

Subtracting $n + n_0$ from $2n_0$ yields the final version of the equation, as shown in the figure. The reason for this is that c/N can be swapped for M/NA in dilutions. We may now express the dispersion of a polymer molecule using this phrase:

$$\frac{i}{I_o} = \frac{2\pi^2 n_0^2 (dn/dc)^2 M^2 \left(1 + \cos^2 \theta\right)}{\lambda^4 r^2 N_A^2}. \tag{25}$$

Through multiplying it in $N = \text{cNA}$, the scattering of N particles in volume unit would be obtained:

$$\frac{i}{I_o} = \frac{2\pi^2 n_0^2 (dn/dc)^2 Mc \left(1 + \cos^2 \theta\right)}{\lambda^4 r^2 N_A}. \tag{26}$$

Soluble molar mass and mass in unit amount are key factors in determining how much light a substance scatters and how much light a substance scatters, according to this equation.

The passing beam modest depth from a polymer solution may be measured in a simple check. The lack of intensity could be caused by scattering if just a little amount of the mild is absorbed. I integer is used to calculate the universal scattering intensity. From this formula, the passing mild depth can be determined:

$$I = I_0 e^{-\tau x}, \tag{27}$$

where t is the turbidity and x is the cell thickness in the direction of the incident beam. This is one form of the Beer law for light weakening. The calculations result in the following:

$$\tau = \frac{32\pi^3 n_0^2 (dn/dc)^2 Mc}{3N_A \lambda^4} = HMc, \tag{28}$$

where

$$H = \frac{32\pi^3 n_0^2 (dn/dc)^2}{3N_A \lambda^4}, \tag{29}$$

in which the pricing remains the same regardless of wavelength or solvent. Turbidity is directly related to molar mass because of this. When opposed to the osmosis strain method, this process is more beneficial for better molar hundreds since it reduces the negative effects of increased molar mass.

A more accurate way to determine the value instead of relying on the preceding calculation is to use the following expression:

$$\tau = \frac{32\pi^3 n_0^2 (dn/dc)^2 Mc}{3N_A \lambda^4} = HMc. \tag{30}$$

From an experimental standpoint, the dimension of scattering depth, y, of the device, shown in Figure four-5, has a higher sensitivity.

2.6. Polar Nephelometer. Light that is scattered in different directions can be measured with a nephelometer, a tool that does this. In some cases, you can move the detector around the polarised pattern by moving it around (scattering cell).

Among other things, it could be a lamp with a collimator (like tungsten-halogen or mercury-pressure) and a collimator that is absolutely perfect, or it could be a laser that does not need a collimator at all and can be used on its own.

It seems that lasers are not very good at making electricity. They can be found in most photography stores, and they are not too expensive. Because the laser is so efficient and cheap, it is a good choice over lasers that do not protect waves.

2.7. The Dispersion of Light. Absorption and scattering dealers are to blame for the amount of light loss in the extinction sample.

The Bessel feature is used to describe the scattering properties of the sample, taking into account the ratio of particle size to wavelength. The following equation predicts that these homes will be built:

$$S_{\text{scattered}}(I_v, I_h, U, V)_{4\times 1} = \frac{F_{4\times 4} \cdot S_{\text{incident}}\left(I_{v_0}, I_{h_0}, U_0, V_0\right)_{4\times 1}}{k_0^2 r^2}, \tag{31}$$

where the zero subscripts are for input rays. In addition, h subscript is related to light's vertical polarisation and v is related to the horizontal polarisation of light. Here, F is a $4 * 4$ matrix, based on Si and S $*$ that replace i.

$$\left\{ \begin{array}{c} I_v = E_v E_v *; \\ I_h = E_h E_h *; \\ U = E_v E_h * + E_h E_v *; \\ V = i\left(E_v E_h * - E_h E_v *\right); \end{array} \right\}. \tag{32}$$

Thus,

$$\left\{ \begin{array}{l} I_v = |S_1|^2 \dfrac{I_{v_o}}{K_0^2 r^2} \\ \\ I_h = |S_2|^2 \dfrac{I_{h_o}}{K_0^2 r^2} \end{array} \right\}. \tag{33}$$

$S1$ and $S2$ in equation (33) depend upon the morphology of scatterer, which are to be obtained from the May theory. In case the particle's dimensions would be larger than being a dipole, $S1$ and $S2$ would be obtained concerning scattering factor:

$$m = \frac{n - ik}{n_0}, \tag{34}$$

where k is the wavenumber and V is the sample volume, and we have

$$\begin{pmatrix} S_1 & 0 \\ 0 & S_2 \end{pmatrix} = \frac{ik_0^3 (m-1)V}{2\pi} \sqrt{P(x)} \begin{pmatrix} 1 & 0 \\ 0 & \cos\theta \end{pmatrix}. \tag{35}$$

Through multiplying equation (34) by its complex, we have

$$\begin{pmatrix} |S_1|^2 & 0 \\ 0 & |S_2|^2 \end{pmatrix} = -k_0^6 \left(\frac{(m-1)V}{2\pi} \right)^2 P(x) \begin{pmatrix} 1 & 0 \\ 0 & \cos^2 \theta \end{pmatrix}. \tag{36}$$

Through substituting equation (33) in (36), we have

$$\begin{pmatrix} \frac{I_v}{I_{v_0}} & 0 \\ 0 & \frac{I_h}{I_{h_0}} \end{pmatrix} = \frac{k_0^4}{r^2} \left(\frac{(1-m)V}{2\pi} \right) P(x) \begin{pmatrix} 1 & 0 \\ 0 & \cos^2 \theta \end{pmatrix}. \tag{37}$$

The scattering factor might be simply calculated by treating r as a constant distance and knowing the intensities arriving at the detector from various angles.

2.8. Experimental Setup. The polarisation modes needed to measure the intensity of silver nanoparticle-spread light have been unique. It was planned in the first step, when a lamp with a full range of visible wavelengths was used. Silver nanoparticles would be able to absorb the light at a certain depth, which was thought about. In that way, the detector was set up to match the mild supply sample, and different wavelengths were pumped into the sample field when it moved. To do this, a sample solvent has also been used.

(a) Scattering visible spectrometer components can be assembled using a variety of methods.

(b) In an array spectrometer, the mild source can be replaced with another mild source, or the polychromator and detector can be replaced.

(c) Modification of the nonarray spectrometer's mild delivery and polychromator

(d) Nonarray spectrometer detectors that are moved. These modes are evident in Figure 3.

2.9. Parts of the Devices That Were Made

2.9.1. Light Source. All visible wavelengths (300–700 nm) are produced with excessive depth by the observed mild source. It is a low-voltage halogen lamp with an incandescent metallic filament. Because an incandescent bulb is heated to a temperature approaching to 500°C, it should produce an enormous amount of light. This lamp is powered by a modern-day trans. City energy is the entry point for this trans. As a safety precaution, three character fans are used to keep it cool. A concave mirror at the bottom of the lamp's lower back and a pair of lenses at its front might be used to focus some of the light produced by this lamp outside of the lamp casing.

2.9.2. The Grating and its Operator. One possibility is that the 1200-line diffraction grid might be able to break down some of the centre and extra light from the lamp into

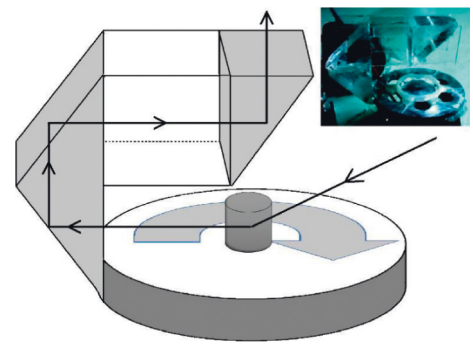

Figure 3: Different ways we could make and develop the scattering spectrophotometer [6].

wavelengths between 300 and 700 nm. Great waves would arrive on time and in the right place in relation to the sample at hand if a grating operator was in charge of them. A clock engine is a person who works like this.

2.9.3. Cylindrical. The entire casing wall is covered with 31 rows of sensors, each with four light-sensitive sensors. In this cylindrical case, the sample can be placed exactly in the middle and be exposed to the incident wavelengths of light by using a tumbler container. The pattern on the sample can absorb or scatter photons after it has been exposed to a large concentration of mild photons. It is also possible to record the scattered light from the surrounding environment with these detectors. Using a digital multimeter, a passing slight might be recorded by an alternate detector and sent to a computer. The photovoltaic cells are utilised in all other detectors to determine the direction of energy.

Because of its direct course, light enters the detector casing and splits it into two separate cylinders, which must be done in order to reach the end point. In front light (optical hollow) and the ultimate element (zero angle) that we view, there are a total of 118 levels of perspective. For each of the 100 80-step phases, we would alert each one. When using the device's image-resistance software, it may be essential to detect the light emitted by the pattern. As long as we have silver nanoparticles in the same area as the sample for recording the shadowgraph depending on the wavelength, we can use no mind-set sensor for the reference sample function. When plotting silver nanoparticle absorption, it is generally best to deduce the silver solution-introduced roughly dark from the precipitation-induced dark. Silver nanoparticles have been exhibited in the graphs that indicate lighting fixtures that were blocked from entering the detector. As long as the photodiode has zero perspective, the graph can also represent the intensity of the passing medium in terms of wavelength if a reference is placed at the sample site. Inverting the graph, the reference-triggered darkness distance can be determined. This method may be used to analyse silver nanoparticles, and the absorption graph can be derived from their darkness graph by comparing it to a reference darkness graph.

Each half of the cylinder is probably divided into 100 and 80°, as was previously mentioned (the use of a protractor). In

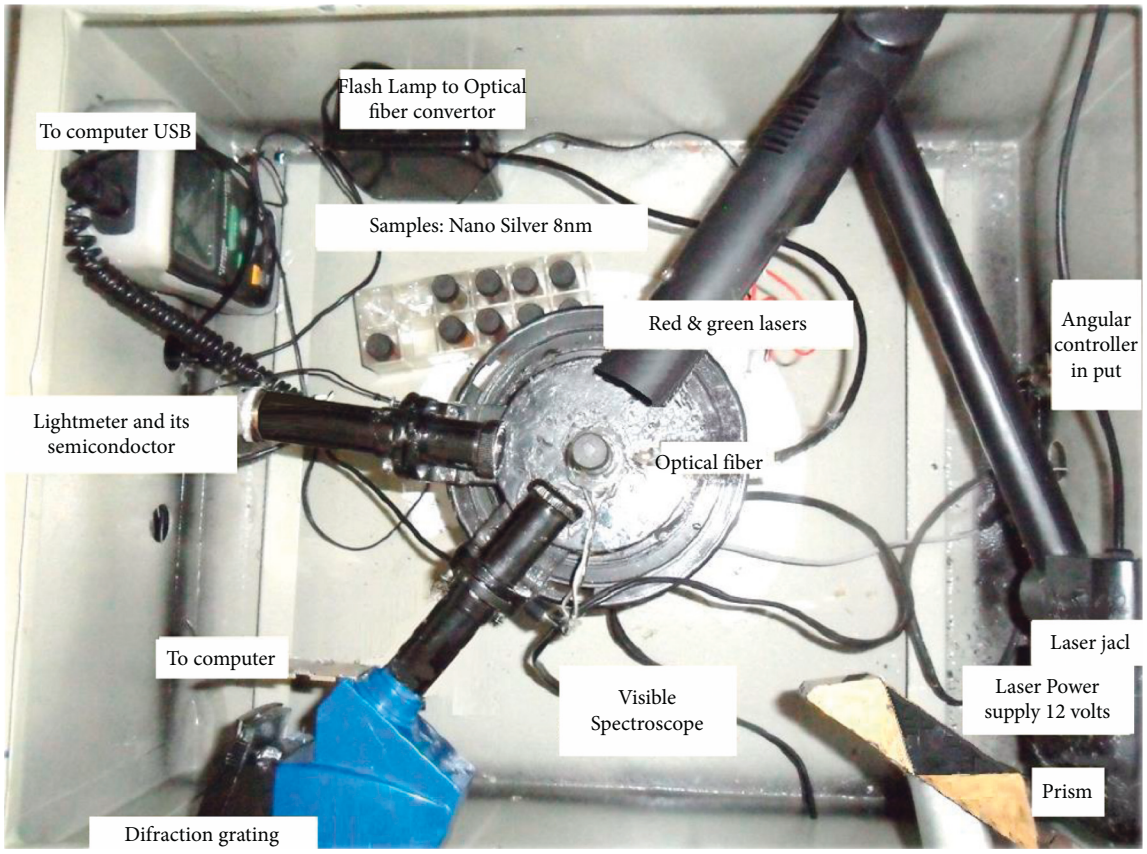

Figure 4: The 5th and most advanced device to date; it features a white LED light and lasers in green and red [8].

primary mode, the multimeter can receive a signal from any of the ten available ranges. This is a manual procedure. Following an examination of the first ten levels, we proceed to the next ten levels and replace the wires until all one hundred seventy tiers can be recorded in the laptop (the final ten tiers do not belong to picture resistance because of the entrance hole).

2.9.4. Remove the Polariser Filter. An additional polariser is introduced before and after the sample to enhance polarised light. When an engine's ball bearings are used, this cleaning procedure can provide a flexible and precise rotation.

2.9.5. Prism Enhancing Agents. As a result, revolving prisms were utilised to reflect both inbound and outbound rays.

2.10. Scattered-Spectrophotometry Integration. To begin, a vintage video projector was used as a light source, and a 1200 diffraction mesh was employed to separate the wavelengths, with a photocell serving as a detector. An urban tungsten light was employed during the second setup attempt as a moderate supply in the metal hole space. Ziman test's CCD has been used to assess the unique spectral patterns created by the scattering of light from the spectroscope's spectrometer. There are no changes to the other components except for the detector, which uses 360-tiers array photoresistance for sample evaluation. Additionally, a photodiode was employed for pattern evaluation in the fourth attempt.

In addition, a mild metre and a spectroscope gadget have been utilised to rotate the sample 360°. In order to be able to link to a computer, the specified mild metre was changed. A few types of electric-powered engines have also been used to move the detector arm in a variety of ways.

3. Results

The results are discussed in Figure 4. The patterns went in and out wards of LED. This method has been used for a long time (in reality at the same time as the sample solvent, e.g., distilled water, which is also called a reference, is placed within the casing). When you do this, you will fix all of the mistakes that come from the sample subject and other things, such as spelling mistakes. The truth is this could be done. It can also be used to get different results based on the angle and wavelength of the light that it emits.

First, we'd place the reference, and then, we'd expand the matrix. Then, we'd put the nanoparticle in and get a new matrix. It's our goal to figure out how far the light is scattered, so we need a way to figure out how far the light is scattered with the help of the nanoparticle. This is how we do it: the results may be shown in Excel software in a symmetrical way.

It would look like this if the same sample were put in a spectrophotometer that was calibrated.

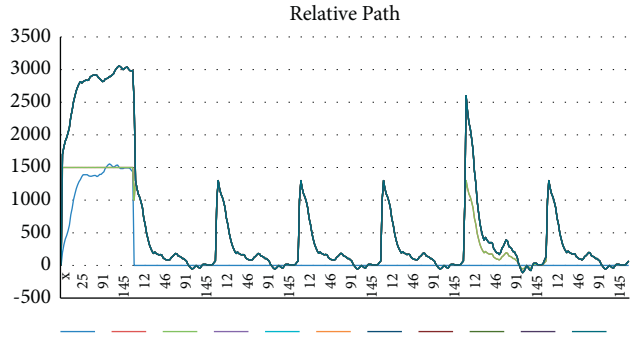

Figure 5: Work under 15 different wavelengths and 155 different angles [4].

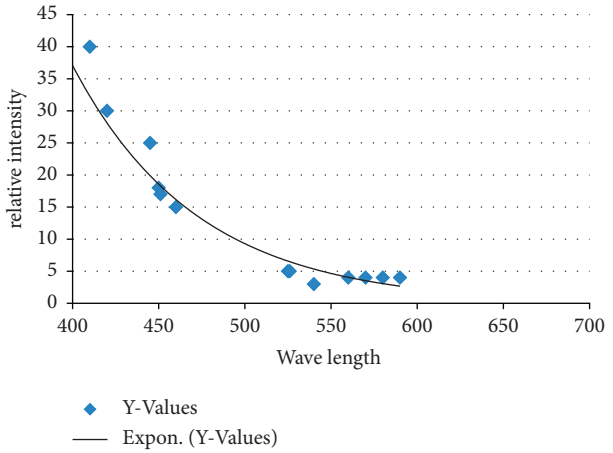

Figure 6: When the silver nanoparticles and water were placed at the same angle, this picture shows the difference in intensity between them [5].

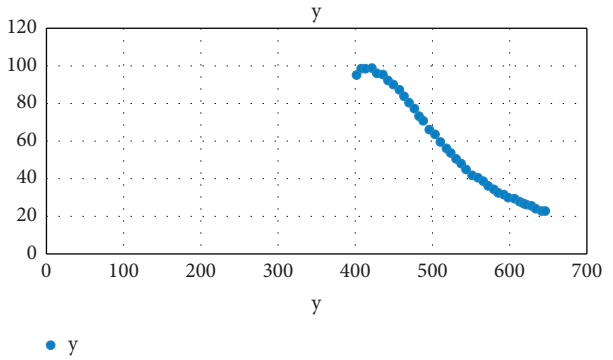

Figure 7: Silver nanoparticles are absorbed by a UV-Vis spectrophotometer that has been calibrated [7].

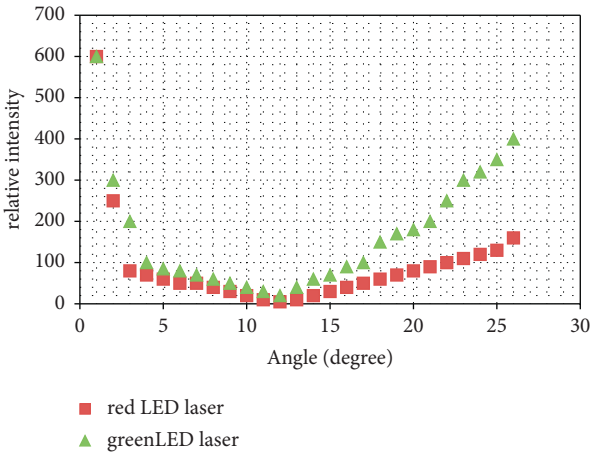

Figure 8: Silver nanoparticles disperse the intensity of green and red laser diode photons in diverse directions [8]. Polarisation has also been examined in a separate investigation. Once the polarised light enters the sample, a polariser blade is placed back into the pattern's path following polarisation scattering. While the second polariser was rotating at an unusual angle, Excel software was used to represent the final intensity in a variety of wavelengths.

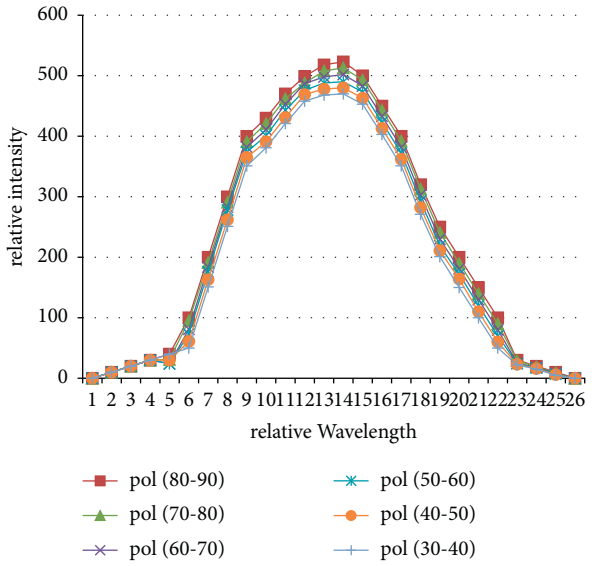

Figure 9: An examination of the arriving light intensities in six polarisations at zero angle. The wavelength is shown on the horizontal axis [7].

Two algebra sentences that came from Excel software would be broken down by their drawings. We would get a sentence that can be used to calibrate our spectrophotometer after we did it this way:

$$G = \frac{10^{-9}x^5 - 3 \times 10^{-6}x^4 + 3.2 \times 10^{-3}x^3 - 1.8x^2 + 501.72x - 54972}{-6 \times 10^{-6}x^5 + 5 \times 10^{-4}x^4 - 1.56 \times 10^{-2}x^3 + 0.2532x^2 - 2.0385x + 6.7128}. \quad (38)$$

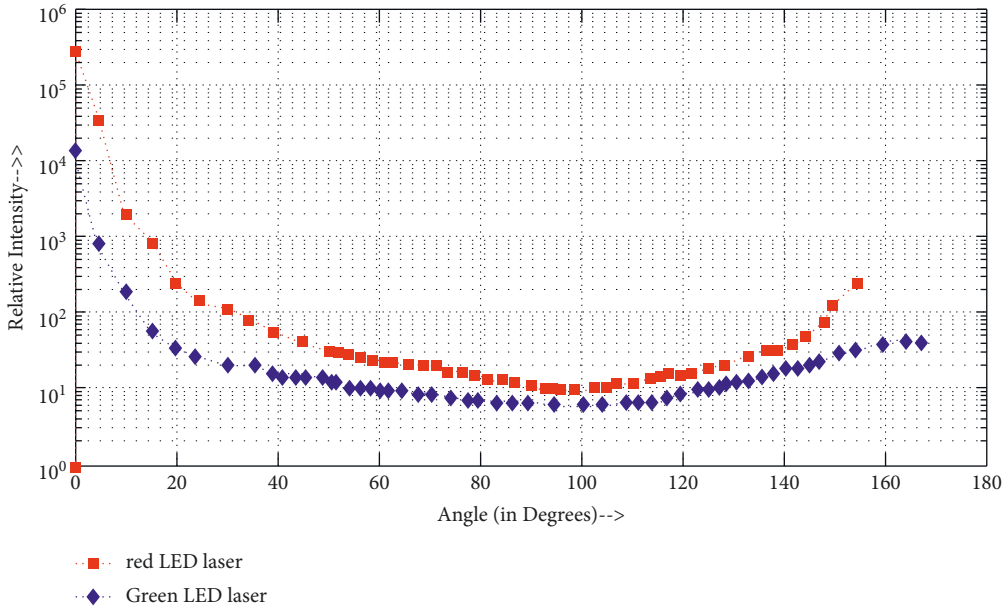

Figure 10: Cellular scattering curves obtained under 12 different 1000-nm light angles, with the black line being the mean [6].

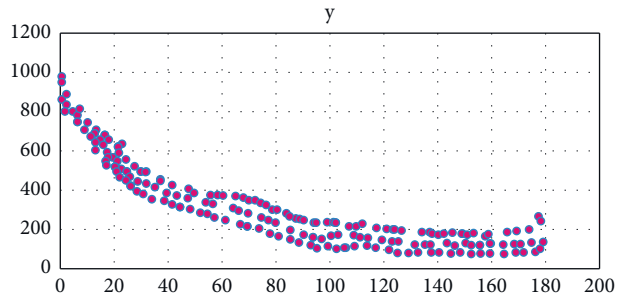

Figure 11: When the crust is taken into account, the scattering spectrum for globes with a radius of 13.4 micrometres is 14.5 micrometres [6].

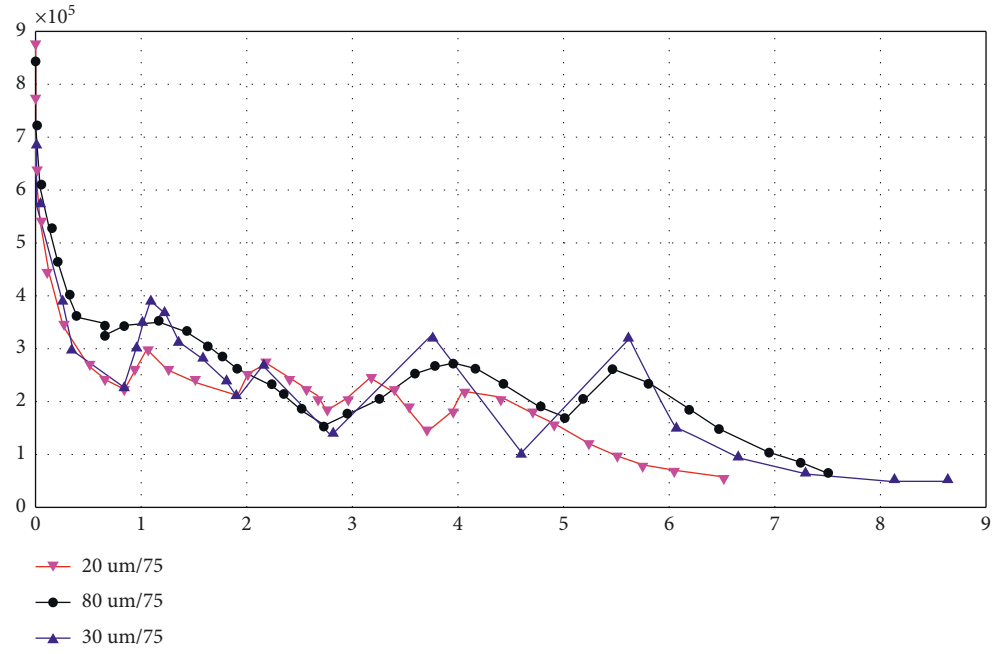

Figure 12: Three distinct hexagonal nanoparticles were used to create a scattering curve [7].

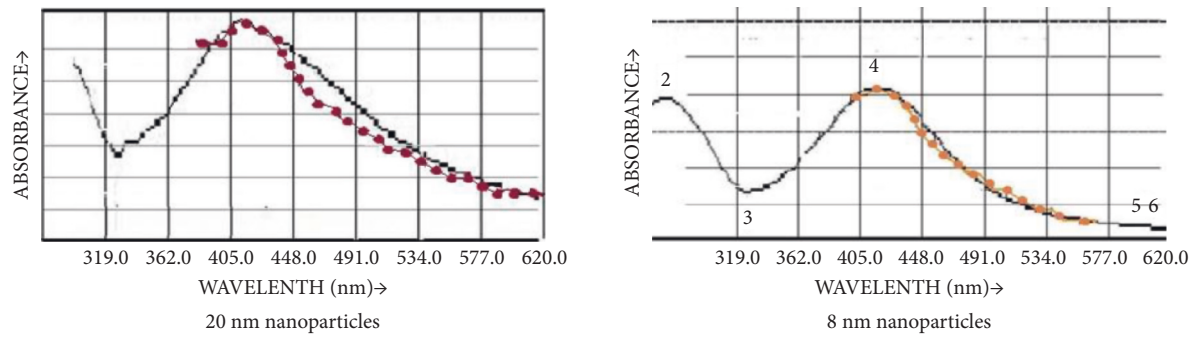

Figure 13: Experimental data from an advanced device (dashed lines) and reference values for a Vis spectrum of 8- and 20-nm silver nanoparticles are shown to be in good agreement [9].

After passing through silver nanoparticles, the light emitted by a green and pink laser diode has been shown in Excel software programme in various instructions and based on Lux.(Figures 4–9)

4. Discussion

A comparison to other studies is made in the study. Polarised nephelometers are used in Figure 10 to study cells under 12 polarisations and 180 rotations of the nephelometer. The advantages of using a polarised nephelometer over a standard nephelometer for membranous material testing are obvious.

Figure 11 depicts the scattering spectrum's dependency on the incoming wavelength in angles greater than zero degrees. Hexagonal nanoparticles can be predicted by their scattering spectrum, which is shown in Figure 12.

5. Conclusion

It is possible to determine the types and concentrations of chemical solutions using visual spectrophotometry. Inside nanoscale solutions, the length of nanoparticles can also be measured. The size of nanoparticles can be estimated in a variety of methods based on their morphology and shape by measuring the depth of mild passing through the nanoparticle solution. This is based on theories like Mueller's scattering matrix, as well as relevant tests. Based on the most recent three-dimensional diagrams, it is possible to anticipate the form and composition of nanoparticles in a solution. In comparison with other methods for determining morphology, I would choose this method as a less expensive alternative to electron microscopy. It is a 3D scanner with a twist: the pattern beneath examination is fluid, rather than solid, and it may deliver high-precision results for outdoor designs. Similar to a 3D scanner, visible lights can be blasted at the sample. After taking a photo of the moderate reflected by the sample and calculating its wavelength in a computer, the researcher was able to learn more about nanoparticles (Figure 13).

Because of the scattering of nanoparticles, the direction of number one intensity, the wavelength of incident light, and polarisation should be influenced by their detection. Researchers will gain valuable information about the nanoparticles' cloth, morphology, and size by conducting this experiment. There are no UV-Vis absorption spectrophotometers that have those kinds of features.

Data Availability

The data used to support the findings of this study are included within the article. Should further data or information be required, they are available from the corresponding author upon request.

Conflicts of Interest

The authors declare that there are no conflicts of interest regarding the publication of this article.

Acknowledgments

The authors thank Koneru Lakshmaiah Education Foundation, Vijayawada, and Addis Ababa Science and Technology University, Ethiopia, for providing characterisation support to complete this research work.

References

[1] Principles of nano-optics (1st volume); lukas nootny; brett hasht; translation by mohammadhossein majlesara; markaz nashr-e-daneshgahi.
[2] P. J. Isaac, "Synthesis of Zeolite/activated carbon composite material for the removal of lead (ii) and cadmium(ii) ions," *Environmental Progess and Sustainable Energy*, vol. 38, no. 6, Article ID e13246, 2019.
[3] J. David, *Electrodynamics*, John Wiley, Hoboken, New Jersy, USA, 2013.
[4] Q. Mechanics, First volume; franz schwabl.
[5] P. Chemistry, First Edition, Robert A.Alberty, Robert J. Silbey.
[6] X. U. Renliang, *Particle Characterization Light Scattering Methods*, Kluwer Academic Publishers, Alphen aan den Rijn, Netherlands, 2019.
[7] J. Connell, "Angle-resolved Mueller matrix study of light-scattering by B-cells at three wavelengths," *Analytical Chemistry*, vol. 442, no. 633, p. 850, 2016.
[8] R. Lawless, Y. Xie, P. Yang- George, and W. Kattawar, "Polarization and effective Mueller matrix for multiple scattering of light by nonspherical ice crystals," 2013.
[9] T. F. Cullen and S. R. Crouch, "Multicomponent kinetic determinations using multivariate calibration," *Mikrochimica Acta*, vol. 126, no. 1-2, pp. 1–9, 1997.